

Document downloaded from:

<http://hdl.handle.net/10251/147619>

This paper must be cited as:

Quelal-Vásconez, MA.; Pérez-Esteve, É.; Arnau-Bonachera, A.; Barat Baviera, JM.; Talens Oliag, P. (2018). Rapid fraud detection of cocoa powder with carob flour using near infrared spectroscopy. *Food Control*. 92:183-189. <https://doi.org/10.1016/j.foodcont.2018.05.001>



The final publication is available at

<https://doi.org/10.1016/j.foodcont.2018.05.001>

Copyright Elsevier

Additional Information

1 **Rapid fraud detection of cocoa powder with carob flour using near infrared spectroscopy**

2

3 Maribel Alexandra Quelal-Vásconez^a, Édgar Pérez-Esteve^a, Alberto Arnau-Bonachera^{b,c}, José

4 Manuel Barat^a, Pau Talens^{a*}

5 ^a *Departamento de Tecnología de Alimentos. Universitat Politècnica de València.*

6 *Camino de Vera, s/n 46022, Valencia, Spain*

7 ^b *Institute for Animal Science and Technology. Universitat Politècnica de València.*

8 *Camino de Vera, s/n 46022, Valencia, Spain*

9 ^c *Biomedical Research Institute (PASAPTA-Pathology group), Veterinary School,*

10 *Universidad Cardenal Herrera-CEU, CEU Universities, Av. Seminario s/n, 46113*

11 *Moncada, Valencia, Spain*

12

13 * Corresponding author: pautalens@tal.upv.es

14

15 **Abstract**

16 Cocoa powder is a highly valuable global product that can be adulterated with low-cost

17 raw materials like carob flour as small amounts of this flour would not change the color,

18 aroma and taste characteristics of the final product. Rapid methods, like NIR technology

19 combined with multivariate analysis, are interesting for such detection. [In this work,](#)

20 [unaltered cocoa powders with different alkalization levels, carob flours with three](#)

21 [different roasting degrees, and adulterated samples, prepared by blending cocoa](#)

22 [powders with carob flour at several proportions, were analyzed.](#) The diffuse reflectance

23 spectra of the samples of 1100 - 2500 nm were acquired in a Foss NIR

24 spectrophotometer. A qualitative and a quantitative analysis were done. For the

25 qualitative analysis, a principal component analysis (PCA) and a partial least squares

26 discriminant analysis (PLS-DA) were performed. Good results (100% classification

27 accuracy) were obtained, which indicates the possibility of distinguishing pure cocoa
28 powders from adulterated samples. For the quantitative analysis, a partial least squares
29 (PLS) regression analysis was performed. The most robust PLS prediction model was
30 obtained with one factor (LV), a coefficient of determination for prediction (R_P^2) of
31 0.974 and a root mean square error of prediction (RMSEP) of 3.2% for the external set.
32 These data allowed us to conclude that NIR technology combined with multivariate
33 analysis enables the identification and determination of the amount of natural cocoa
34 powder present in a mixture adulterated with carob flour.

35 *Keywords: Cocoa powder, adulteration, carob flour, NIR, PCA, PLS.*

36 1. Introduction

37

38 Cocoa powder, thanks to its characteristic and pleasant flavor and aroma, is one of
39 the most valued commodities around the world (Bonvehí, 2005). Among its applications
40 in the food industry, the formulation of beverages, confectionery, bakery and pastry
41 products stands out (Shankar, Levitan, Prescott, & Spence, 2009). Apart from flavor and
42 aroma, cocoa is highly appreciated as a natural coloring agent, partly because of the
43 current tendency to restrict the use of artificial colors.

44 During cocoa processing, it is possible to modify cocoa color and aroma through
45 roasting and/or alkalization processes. Roasting consists of exposing cocoa beans to
46 temperatures of 130–150°C for 15–45 min. It is used to inactivate microorganisms and
47 to develop the characteristic brown color, mild aroma and texture of commercial natural
48 beans (Bonvehí, 2005; Krysiak, 2006; Afoakwa, Budu, Mensah-Brown, Felix & Ofosu-
49 Snsah, 2014). Alkalization is an optional operation to reduce acidity, bitterness and
50 astringency, and to darken cocoa's color. This procedure involves using an alkali
51 (generally potassium carbonate) in combination with oxygen, water and high
52 temperatures. These extreme conditions provoke, among others, Maillard reactions and
53 polyphenol oxidations and polymerizations, which end up with flavor and color
54 modifications from light brown (natural) to red, dark brown or extremely black (Miller
55 et al., 2008; Li et al., 2012).

56 In recent years, the demand for cocoa powder has increased and its supplies have
57 tightened, thus its price has steadily grown (Fadel, Mageed, Samad, & Lotfy, 2006).
58 Consequently, there is a demand to develop cocoa substitutes. Some studies suggest that
59 cocoa-like aromas can be found in roasted carobs (Arrighi, Hartman & Ho, 1997).
60 Carob pods are characterized by a high sugar content (around 50%), composed

61 essentially of sucrose. This high sugar content favors the same chemical reactions that
62 occur during the roasting and alkalization of cocoa: caramelization of high sugar content
63 and Maillard reactions between amino acids and sugars (Fadel et al., 2006). In this way,
64 toasted carob can provide similar aromas to cocoa.

65 Bearing in mind this striking aromatic and visual similarity between carob flour
66 (natural or toasted) and cocoa (natural or alkalized), some traders have seen that selling
67 carob (average price of 940 US\$/tonne) as cocoa (1945 US\$/tonne), by omitting this
68 substitution, is a profitable option to increase their benefits (ICCO, 2017). However,
69 this deliberate, intentional and undeclared substitution of one product for another with a
70 lower price is food fraud that not only affects producers and consumers, but also the
71 physico-chemical properties of the manufactured product. Some studied examples
72 comprise milk chocolates and chocolate cakes, in which some percentages of cocoa
73 powder have been substituted for carob flour (Salem & Ohaad Fahad, 2012; Rosa,
74 Tessele, Prestes, Silveira, & Franco, 2015).

75 To detect food adulteration, the three most widespread technologies are liquid
76 chromatography, infrared spectroscopy and gas chromatography (Moore, Spink, &
77 Lipp, 2012). Liquid and gas chromatography analyses need long sample preparation
78 times, method optimization, and high-cost materials and reagents, while infrared
79 spectroscopy is fast, reliable, less expensive and a chemical-free alternative (Ellis et al.,
80 2012). Near infrared spectroscopy (NIR) is an infrared spectroscopy type characterized
81 by recording reflectance or transmittance spectra within the region from 750 nm to 2500
82 nm. These spectra act as a 'fingerprint' that is characteristic of a particular sample
83 molecule and allows its identification. Some examples of using NIR and multivariate
84 analyses in the cocoa sector include the prediction of basic food components, such as
85 moisture, carbohydrate, fat, protein, theobromine and catechin and total polyphenol

86 content (Veselá et al., 2007; Álvarez et al., 2012; Huang et al., 2014). In other sectors,
87 NIR in combination with a multivariate analysis has been employed to detect starch in
88 onion powders, acid whey, starch, maltodextrin in skim powder milk, sudan dyes in
89 chili powders, and talcum powder in teas (Lohumi, Lee, Lee, & Cho, 2014; Capuano,
90 Boerrigter-Eenling, Koot, & van Ruth, 2015; Haughey, Galvin-King, Ho, Bell, &
91 Elliott, 2015; Li, Zhang, & He, 2016).

92 In this context, the aim of this work was the rapid detection of the adulteration of
93 cocoa powders, regardless of their alkalization level, with carob flours by applying NIR
94 and a multivariate analysis.

95

96 **2. Materials and Methods**

97

98 *2.1 Raw materials*

99 In order to analyze a good representative set of samples of the variability in
100 commercial cocoa and carob flour, cocoa powders with different alkalization levels
101 (n=12), as well as carob flour powders with three different roasting degrees (n=6) were
102 used in this study. The samples used were natural cocoa (NC), lightly alkalized cocoa
103 (LAC), medium alkalized cocoa (MAC), strong alkalized cocoa (SAC), light carob flour
104 (LCF), medium carob flour (MCF) and dark carob flour (DCF).

105 OLAM Food Ingredients, Spain (Chestre, Valencia), kindly donated cocoa powders.
106 Carob flour powders were bought from a local specialized supermarket. Raw samples
107 were placed inside a glass container and stored in a dry dark atmosphere until were
108 used.

109

110 *2.2 The physico-chemical characterization of raw materials*

111

112 Each of the raw samples was characterized according to their extractable pH value
113 and extrinsic colour. All measurements were taken in triplicate. For extractable pH
114 determination, the process described in The Zaan Manual (Olam, 2017) was followed.
115 For that purpose, 10g of cocoa powder were suspended in 90 mL of boiling distilled
116 water and stirred. After decreasing temperature to 20-25°C in a cold bath, sample pH
117 was measured with a digital pH-meter (Crison Instruments, S.A., Barcelona, Spain)
118 previously calibrated with 3 buffer solutions: pH 4.01, pH 7.0 and pH 9.21 (T=25 °C).
119 According to pH value, samples were classified in four different categories: natural
120 cocoa powders (5< pH<6), light alkalized (6<pH<7.2), medium alkalized (7.2< pH<7.6)
121 and strong alkalized powders (pH >7.6) (Miller et al., 2008).

122 To determine the extrinsic color, a cocoa powder sample was placed in a
123 methacrylate cuvette by unifying the degree of compaction through small successive
124 shocks. Color was measured in a spectrophotometer Minolta CM 3600D (Tokyo,
125 Japan). Reflectance spectra (between 400 - 700 nm) were used to obtain color
126 coordinates L*, a* and b* for D65 illuminant and 10° observer. Hue (h^*) and chroma
127 (C^*) were estimated by Equation 1 and Equation2, respectively.

128

129
$$h^* = \arctg \frac{b^*}{a^*} \tag{1}$$

130

131
$$C^* = \sqrt{a^{*2} + b^{*2}} \tag{2}$$

132

133 *2.3 Preparing adulterated samples*

134

135 In this study, two batches of 234 samples composed of 12 unaltered cocoa powders,
136 6 carob flours, and 216 adulterated samples, were used. The adulterated samples were
137 prepared by blending the 12 cocoa powders with the 6 different carob flours at different
138 proportions. For all the 72 possible cocoa-carob combinations, three different levels of
139 adulteration were prepared: low adulteration LA (0-20%), medium adulteration MA
140 (20-40%) and high adulteration HA (40-60%). The upper limit (60%) was set by
141 considering that above this concentration, adulteration would become evident due to the
142 characteristic carob aroma (Cantalejo, 1997). The specific adulteration percentage at a
143 given level was determined randomly from a uniform distribution (each adulteration
144 percentage had the same probability of being selected), following the Latin Hypercube
145 Strategy (LHS) (Helton & Davis, 2003). The adulterated samples were placed in a glass
146 container and stored in a dry dark atmosphere until used.

147

148 *2.4 Collecting near-infrared spectra*

149

150 All samples were scanned, by triplicate, in a FOSS NIR 5000 System
151 spectrophotometer (Silver Spring, MD, USA) equipped with a transport module. Round
152 sample cups (3.8 cm diameter x 1cm thick quartz windows) were filled with each
153 sample (about 5 g) so that the surface and thickness remained uniform during spectral
154 collection. The instrument measures diffuse reflectance and automatically converts it
155 into relative absorbance ($\log 1/R$) to obtain a linear correlation with the concentration of
156 the product's chemical constituents (Martens, Nielsen, & Engelsen, 2003). Thirty-two
157 successive scans with 700 points (wavelengths) from each sample were collected within
158 a wavelength range from 1100 nm to 2500 nm at 2-nm intervals.

159

160 2.5 Chemometric analysis

161

162 An analysis of variance (ANOVA) was used to determine the differences in pH and
163 extrinsic color among samples. Data were statistically processed using Statgraphics
164 Centurion XVI (Manugistics Inc., Rockville, MD, USA). Simultaneously, color
165 parameters C*, h* and L* and pH were used in a principal component analysis (PCA) to
166 show the samples and their relationship. Before the analysis, an autoscaling was
167 performed in order to improve the weights of the variable with small values.

168 A multivariate analysis was conducted by a qualitative analysis and a quantitative
169 analysis by The Unscrambler v10.4 (CAMO Software AS, OSLO, Norway). For the
170 qualitative analysis, a PCA and a partial least squares discriminant analysis (PLS-DA)
171 was performed. The PCA was run with raw data, while the PLS-DA (Berrueta, Alonso,
172 & Héberger, 2007) was constructed after applying spectra 2nd derivative Savitzky-Golay
173 smoothing (2nd derivative S-G) (Savitzky & Golay, 1951) and orthogonal signal
174 correction (OSC). Both pre-treatments were applied to acquire useful information,
175 improve the signal-to-noise ratio and remove systematic variation from the predictor
176 matrix X unrelated, or orthogonal, to matrix Y (Wold, Antti, Lindgren, & Öhman, 1998;
177 Pizarro et al., 2004). For the quantitative analysis, a partial least squares (PLS)
178 regression analysis was performed. In order to evaluate and correct the multiplicative
179 and additive effects caused by different light scattering in the spectroscopic
180 measurement (Cozzolino et al., 2011; Stohner et al., 2012), four PLS models were
181 tested. The PLS were constructed using the raw spectrum and by applying three pre-
182 treatments to the spectrum: 2nd derivative S-G, OSC and the combination of them.

183

184 2.5.1 Developing calibration models

185 Two databases were used for the analysis. The first database consisted of 468 spectra
186 and 700 variables (wavelengths, nm) was used for the PCA and PLS models. For the
187 PLS-DA classification samples were divided into three categories (0=Cocoa;
188 1=Adulterated samples and 2=Carob flour) and a second database with 142 spectra and
189 700 variables was created to balance the number of samples that belonged to each
190 category. Moreover, the spectra of each database were randomly separated into two
191 different data sets. A set with 70% of the spectra was used to create and evaluate the
192 model by leave-one-out cross-validation. The other set, with 30% of the remaining
193 samples, was used for external validation. The relative performance of the constructed
194 models was assessed by the required number of latent variables (LVs), the coefficient of
195 determination for calibration (R^2_C), the root mean square error of calibration (RMSEC),
196 the coefficient of determination for cross validation (R^2_{CV}) and the root mean square
197 error of leave-one-out cross validation (RMSECV). A model can be considered good
198 when a few LVs are required, and when it has low RMSEC and RMSECV and high R^2_C
199 and R^2_{CV} . A cut-off value of ± 0.5 was used for the classification of the samples (Dong,
200 Zhao, Hu, Dong, & Tan, 2017).

201

202 2.5.2 External validation

203

204 To assess the models' predictive capability, the coefficient of determination for
205 prediction (R^2_P), the root mean square error of prediction (RMSEP), the ratio of
206 prediction deviation (RPD = SD/RMSEP), where SD was the standard deviation of the
207 Y-variable in the prediction set, and bias were used. The RPD is more meaningful than
208 only looking at the error of prediction. An RPD value lower than 2 is considered
209 insufficient for application, one between 2 and 2.5 is considered for approximate

210 quantification, and values between 2.5 and 3 are taken as a good model, while models
211 with RPD values above 3 can be considered excellent and most reliable for analytical
212 tasks (Sunoj, Igathinathane & Visvanathan, 2016). The bias estimates the difference
213 between the experimental value and NIR predictions, and can be positive or negative.
214 Positive values indicate that the model overestimates, while negative values suggest
215 otherwise. Higher bias values indicate that NIR predictions vary significantly from the
216 experimental values (Cantor, Hoag, Ellison, Khan, & Lyon, 2011), so it is better if it
217 comes close to zero.

218

219 **3. Results and Discussion**

220

221 *3.1 Raw materials characterization*

222

223 Table 1 contains the color parameters and pH values of the different raw materials.
224 As observed, the obtained pH values ranged from 5.3 (NC1) to 7.9 (SAC3). According
225 to these values and following the Miller Classification, twelve samples were considered
226 natural cocoas (NC; $5 < \text{pH} < 6$), three samples light alkalized cocoas (LAC; $5 < \text{pH} < 6.2$),
227 tree samples medium alkalized cocoas (MAC; $7.2 < \text{pH} < 7.6$) and three samples strong
228 alkalized cocoas (SAC; $\text{PH} > 7.6$). pH can be used as an indicator of the degree of
229 alkalization that occurs during production because the pH value of cocoa powder is
230 related to the amount and type of alkali used in the process (OLAM Cocoa Manual,
231 2017; Pérez, Lerma, Fuentes, Palomares, & Barat, 2016). The inclusion of cocoas with
232 different degrees of alkalization during the model-building phase assures that it might
233 be used with independence of the cocoa powder processing.

234 The **lightness** (L^*) values measured in the cocoa samples ranged from 31 (SAC1) to
235 50 (NC3). The maximum **lightness** value appeared in a NC sample (NC3). The L^* value
236 progressively lowered according to the degree of alkalization to the minimum value in
237 the SAC samples with a very dark color. The differences in the **lightness** in the NC
238 samples (NC1, NC2 and NC3) could be due to a different geographical origin or to
239 distinct processing in the fermentation or roasting stages (Afoakwa, et al., 2014).

240 The chroma (C^*) values oscillated between 11 (SAC1) and 22 (NC2). As seen in
241 Table 1, the higher the alkalization degree, the lower purity becomes.

242 Hue (h^*), unlike the other parameters, does not follow a linear relationship with an
243 increased pH value. Cocoa samples evolve from a more yellow-orange hue ($h^* = 60$) to
244 a more orange-red one ($h^* = 43$) in the alkaline cocoa samples.

245 The pH of carob flours ranged from 4.5 to 5.1, with no trend observed between the
246 pH value and the degree of toasting samples. Thus, carob samples could be added to the
247 NC beans in high proportions without significantly changing the mixture's pH value.

248 The L^* values in the carob flours ranged from 34 (DCF) to 49 (LCF), which meant
249 that **lightness** progressively lowered as the degree of roasting increased. When these
250 values were compared with those of cocoa, were found no statistical differences
251 ($p < 0.05$) between the NC samples and natural carob meal (LCF samples), nor between
252 the **lightness** of MAC and SAC samples and roasted carob (MCF and DCF). These
253 minor differences in **lightness** would favor the adulteration of cocoa with carob meal.

254 The chroma (C^*) of the samples also decreased as the degree of roasting rose, with
255 values of 23.7 for LCF samples that lowered to 13 for strong roasted carob (DCF
256 samples). When comparing the C^* values between cocoa and carob, we found a
257 similarity between both. Thus the C^* values would be the equivalent between natural

258 cocoa and natural carob meal, and between medium/strong cocoa beans and roasted
259 carob.

260 The hue (h^*) values for the carob flours gave no significant differences with an
261 increasing degree of roasting, but only a slight decrease. The values obtained for the
262 carob flour samples were 61 on average. These values coincided with those observed in
263 the NC samples.

264 Cocoa color parameters are generally affected by several factors, including the
265 degree of roasting and alkalization. The strong alkalized ones were dark, while the
266 natural ones were lighter. The roasting result was darkened cocoa or carob due to the
267 formation of brown pigments (Zyzelewicz, Krysiak, Nebesny, & Budryn, 2014), with
268 changes noted in the values of the individual color parameters.

269

270 Insert Table 1 here

271

272 In order to know how the physico-chemical properties explained the different
273 characteristics between the cocoa and carob flour samples, a PCA was performed with
274 the pH and color parameters. Figure 1 shows the two-dimensional scatter plot of scores
275 for two principal components (PCs) from projection results and allows the visualization
276 of the distribution of the scores of the samples of cocoa and carob powder. The two
277 PCs explain over 94% of the variation. The first PC explains 78 % of the variance and is
278 related with the roasted degree of the carob, or alkalization of the cocoa powder,
279 whereas the second PC explains 16 % of the total variance and is related with the
280 difference between level of alkalized cocoa and the carob flour.

281 The natural cocoa NC and light carob flour LCF scores were close, which indicated
282 that these samples were related and had similar pH characteristics and color parameters..

283 The positive scores on component 1 and component 2 corresponded to the samples with
284 different degrees of alkalization. This position and the loading values of the variables
285 led to the conclusion that the samples with low lightness and high pH were the alkaline
286 cacao samples, while the samples with low lightness and low pH were those of roasted
287 carob flour (Dark (DCF) and medium (MCF)). This agrees with the results presented by
288 other authors (Bulca, 2016; Yousif & Alghzawi, 2000), which indicated that carob flour
289 could not be visually separated from cocoa powder, not even when the other groups of
290 the alkalized and roasting samples were blended.

291

292 Insert Figure 1 here

293

294 *3.2 Spectral differences analysis of carob and cocoa powder*

295

296 The spectra of the relative absorbance of cocoa powder and carob flour are
297 represented in Figure 2 (a, b). All the cocoa spectra display a similar absorbance pattern,
298 this pattern differs between cocoa and carob flour in relation to the absorbance intensity.

299

300 Insert Figure 2 here

301

302 Raw data were preprocessed by applying the 2nd derivative S-G and OSC. Examples
303 of the pretreated spectra of cocoa (brown) and carob (gray) are shown in Figure 3. As
304 observed, after this pretreatment the differences between both spectra types became
305 more evident than in the untreated spectra. It can be stated how divergence pointed
306 between both spectra types being located especially in the magnitude of reflectance at
307 1438, 1728, 2312, 2324, 2350 nm. As expected from the compositional differences,

308 between cocoa powder and carob flours, these wavelengths were associated with the
309 vibration of the functional groups that cocoa powder contains like theobromine and
310 caffeine (1728 nm) (Cozzolino et al., 2011), and epicatechin (2312, 2324 nm)
311 (Esteban, González, & Pizarro, 2004; Teye & Huang, 2015).

312

313 Insert Figure 3 here

314 *3.2 Classification model*

315

316 A PCA was performed as a non-supervised learning algorithm with the raw spectra
317 data to evaluate the relationship among samples. Figure 4 shows the score plot of the
318 first two principal components (PC). The first two PC explain 91% of the total variance
319 among the samples. The first PC explains 71% of total variance and might be related to
320 sample processing. The different natural cocoas are found in the negative region,
321 whereas the alkalinized samples are distributed across the negative and positive regions.
322 These differences could be due to alkali, the stage in which it has been alkalized (bean
323 or cake), and the degree of alkalinization that can produce different color changes (red
324 or dark brown) (Miller et al., 2008). The second PC explains 20% of variability and
325 might be related to the percentage of cocoa powder in the sample. Pure cocoa powders
326 are located in the positive region, while pure carob flours are found in the negative
327 region. The samples with different levels of adulteration lie in the middle: low (0-20%),
328 medium (20-40%) and high (40-60%).

329 The wavelengths that corresponded to the highest loading values were 1100, 1464,
330 1936, 2108, 2276, 2330 and 2486 nm for the first PC, and 1116, 1324 1460, 1576, 1728,
331 1914, 1976, 2106, 2262, 2310 and 2494 nm for the second PC. The wavelengths from
332 971 and 1400 nm were related to the ascending part of the water first overtone

333 absorption peak O–H stretching bonds at 1722 nm C-H stretching was also present,
334 which are associated with water and sugar content (Álvarez et al., 2012; Cozzolino,
335 Smyth, & Gishen, 2003; X. Y. Huang et al., 2014; Talens et al., 2013). The wavelengths
336 at 1736 and 2319-2328 nm were related to the absorption of the C–H bonds, CH₃
337 combination and C-C stretching. These are features of fatty acids, proteins and
338 polysaccharides in cocoa powder and could be associated with a fat content of
339 approximately 10-12% (Veselá et al., 2007; Westad, Schmidt, & Kermit, 2008). The
340 absorption bands of 1728, 2108 and 2494 nm coincided approximately with those that
341 were used to predict the total fat content in cocoa beans by (Ribeiro, Ferreira, & Salva,
342 2011; Teye & Huang, 2015). Variations were related to the compositional
343 characteristics of the cocoa categories and the adulterant carob powder. The found
344 wavelengths were similar to a study performed in cocoa beans (Teye et al., 2015b).
345 Therefore, absorption in wavelengths (as a result of vibrational reactions) contains
346 chemical information that helps explain the observed differences between the carob and
347 cocoa powder pure samples and their several adulteration proportions.

348 Since the generated spectra correspond to an adulteration level on a continuous scale,
349 it was not possible to see well-separated groups (high, medium and low adulterated) in
350 this PCA, especially for the percentages that fell within the limits. With this
351 information, a PLS-DA analysis was created to generate a model with categorized
352 spectra, which allowed the detection of gross adulterations levels.

353

354 Insert Figure 4 here

355

356 As the PCA was unable to see samples in the different groups according to their
357 adulteration percentages, a qualitative model that used the supervised PLS-DA was

358 employed. In order to improve the model's accuracy, the original spectra were pre-
359 processed using 2nd derivative S-G (9-point window, second-order polynomial) and an
360 OSC. For the PLS-DA (Figure 5), three latent variables (LVs) were generated with most
361 of the variation (67%) explained by the first LV and 12% by the second. In this way,
362 separation was achieved mainly by using the first latent variable with the most negative
363 scores for the pure cocoa samples, and the most positive scores related to the adulterate
364 samples and carob powder (pure adulterant). In visually terms, the scores plot
365 differences among the 100% cocoa powder, adulterated cocoa powders and 100% carob
366 powder indicated the possibility of using this approach to quickly screen for
367 adulteration. The determination coefficient (R^2) of this PLS-DA model was 0.969. The
368 cross-validation determination coefficient (R^2_{CV}), based on full cross-validation, was
369 0.901. Those values indicate the goodness of the classification model.

370

371  Insert Figure 5 here

372

373 In order to measure the robustness of the PLS-DA model, validation with an external
374 data set was performed. Table 2 shows the model's capability to classify 100% of the
375 samples in their corresponding groups (cocoa, carob or adulterated samples).

376

377  Insert Table 2 here

378

379 *3.3 Adulterant Prediction*

380

381 A PLS was performed with the calibration set. The prediction was done with the
382 validation set. The models were constructed by applying different pre-treatments to the

383 spectra. The statistical indicators of the goodness of fit of each model are presented in
384 Table 3.

385 Insert Table 3 here

386
387 Good models were obtained with high R^2 values and low RMSE values for the
388 calibration, cross-validation and prediction, depending on spectral data processing. The
389 RPD values were higher than 3, which meant that all these models, even the model
390 without the preprocessing data, could be considered excellent and most reliable for the
391 analytical tasks. This indicated that the multiplicative and additive effects in the spectra
392 of cocoa powder, and with the equipment used for the measurements in this study, were
393 minimal due to even the model without pretreatment to correct that effects was
394 excellent. However, it is important to point out that the models with pre-treatments
395 obtained a smaller number of LV, which made the model more parsimonious. Figure 6
396 presents the observed (x axis) *versus* predicted (y axis) values. The predicted values
397 were obtained with a model that used 2nd Derivative S-G and OSC. We can observe that
398 the PLS algorithm predicted very well with an R_{CV}^2 of 0.979 and an RMSECV of
399 2.897%. The prediction of the external validation group gave a low RMSEP of 3.237%
400 and an R_p^2 of 0.974. The similarity among RMSEC, RMSECV and RMSEP indicated
401 that the possibility of over-fitting the model was very low and confirmed its good
402 prediction capacity. The 2nd derivative S-G and the OSC pretreatment improved the
403 RPD, which was 35.48% higher compared to the PLS model with the raw data, and
404 used only one latent variable (LV). Other studies have found good models with one LV
405 when orthogonal signal correction was used (Esteban et al., 2004). The relative
406 notorious improvement of the RPD in the pretreated model could be due to the NIR
407 signal being affected by environmental (moisture) and physical factors (product's

408 particle size distribution). According to Huang et al., those factors generated light
409 scattering and, consequently, significant differences arose. Additionally, these factors
410 affect the effective sample pathlength and result in additive, multiplicative and
411 wavelength-dependent effects. In some cases, wavelength-dependent scattering is
412 related with baseline shifts, tilt or curvature scaling variation. In certain instances,
413 spectra variations mask any subtle chemical variation, which can produce inaccurate
414 results. Thus pretreatment is effective for cushioning the aforementioned effects (Huang
415 et al., 2010).

416

417

Insert Figure 6 here

418

419 **4. Conclusions**

420 Near infrared spectroscopy (NIR) combined with PLS-DA and PLS statistical
421 models has been shown to be a rapid effective method to identify adulterations of cocoa
422 powder with Carob flour, regardless of the alkalization or roasting level. In contrast,
423 these adulterations would not be readily detectable by routine techniques such as
424 determination of pH analysis and color measurement.

425 With the PLS-DA analysis, all (100%) the samples were correctly classified into
426 three groups: cocoa, carob flour and mixtures. The PLS analysis enabled the percentage
427 of adulteration to be calculated with the samples. The PLS model was obtained with one
428 factor with an R^2 of 0.979 and 0.974, and a mean squared error of 2.9 and 3.2 for the
429 calibration and external validation sets, respectively.

430 This [technique](#) is, therefore, an important tool for cocoa merchants, who will be able
431 to better control the product's quality by avoiding the use of destructive techniques that
432 require complex sample preparations or techniques that imply much expense for

433 companies. Given the excellent results obtained, we expect this method to become
434 increasingly important in the cocoa industry and to reduce food fraud.

435

436 **Acknowledgments**

437 The authors wish to acknowledge the financial assistance provided by the Spanish
438 Government and European Regional Development Fund (Project RTC-2016-5241-2).
439 Maribel Quelal Vásconez thanks the Ministry of Higher Education, Science,
440 Technology and Innovation (SENESCYT) of the Republic of Ecuador for her PhD
441 grant. The Olam Food Ingredients Company is acknowledged for providing part of the
442 cocoa samples used herein.

443

444 **References**

- 445 Afoakwa, E. O., Budu, A. S., Mensah-brown, H., Felix, J., & Ofoosu-ansah, E. (2014).
446 Effect of Roasting Conditions on the Browning Index and Appearance Properties of
447 Pulp Pre-Conditioned and Fermented Cocoa (*Theobroma Cacao*) Beans. *J Nutrition*
448 *Health Food Sci*, 2(1), 1–5.
- 449 Álvarez, C., Pérez, E., Cros, E., Lares, M., Assemat, S., Boulanger, R., & Davrieux, F.
450 (2012). The use of near infrared spectroscopy to determine the fat, caffeine,
451 theobromine and (–)-epicatechin contents in unfermented and sun-dried beans of
452 Criollo cocoa. *Journal of Near Infrared Spectroscopy*, 20(2), 307.
- 453 Arrighi, W. J., Hartman, T. G., & Ho, C. T. (1997). Carob bean aroma dependence on
454 roasting conditions. *Perfumer & flavorist*, 22(1), 31-41.
- 455 Berrueta, L. A., Alonso, R. M., & Héberger, K. (2007). Supervised pattern recognition
456 in food analysis. *Journal of Chromatography A*, 1158(1–2), 196–214.
- 457 Bonvehí, J. S. (2005). Investigation of aromatic compounds in roasted cocoa powder.

458 *European Food Research and Technology*, 221(1–2), 19–29.

459 Bulca, S. (2016). Some properties of carob pod and its use. *Scientific Bulletin. Series F.*
460 *Biotechnologies*, Vol. XX, 142–147.

461 Cantalejo, M. J. (1997). Effects of Roasting Temperature on the Aroma Components of
462 Carob (*Ceratonia siliqua* L.). *Journal of Agricultural and Food Chemistry*, 45(4),
463 1345–1350.

464 Cantor, S.L., Hoag, S.W., Ellison, C.D., Khan, M.A., Lyon, R.C., 2011. NIR
465 spectroscopy applications in the development of a compacted multiparticulate
466 system for modified release. *AAPS PharmSciTech* 12, 262–278.

467 Capuano, E., Boerrigter-Eenling, R., Koot, A., & van Ruth, S. M. (2015). Targeted and
468 Untargeted Detection of Skim Milk Powder Adulteration by Near-Infrared
469 Spectroscopy. *Food Analytical Methods*, 8(8), 2125–2134.

470 Cozzolino, D., Smyth, H. E., & Gishen, M. (2003). Feasibility Study on the Use of
471 Visible and Near-Infrared Spectroscopy Together with Chemometrics to
472 Discriminate between Commercial White Wines of Different Varietal Origins.
473 *Journal of Agricultural and Food Chemistry*, 51(26), 7703–7708.

474 Cozzolino, D., Cynkar, W. U., Shah, N., & Smith, P. (2011). Multivariate data analysis
475 applied to spectroscopy: Potential application to juice and fruit quality. *Food*
476 *Research International*, 44(7), 1888–1896.

477 Dong, W., Zhao, J., Hu, R., Dong, Y., & Tan, L. (2017). Differentiation of Chinese
478 robusta coffees according to species, using a combined electronic nose and tongue,
479 with the aid of chemometrics. *Food Chemistry*, 229, 743-751.

480 Ellis, D. I., Brewster, V. L., Dunn, W. B., Allwood, J. W., Golovanov, A. P., &
481 Goodacre, R. (2012). Fingerprinting food: current technologies for the detection of
482 food adulteration and contamination. *Chemical Society Reviews*, 41(17), 5706.

483 Esteban, I., González, J. M., & Pizarro, C. (2004). Prediction of sensory properties of
484 espresso from roasted coffee samples by near-infrared spectroscopy. *Analytica*
485 *Chimica Acta*, 525(2), 171–182.

486 Fadel, H. H., Mageed, M. A. A., Samad, A. K. M. A., & Lotfy, S. N. (2006). Cocoa
487 substitute: Evaluation of sensory qualities and flavour stability. *European Food*
488 *Research and Technology*, 223(1), 125-131.

489 Haughey, S. A., Galvin-King, P., Ho, Y.-C., Bell, S. E. J., & Elliott, C. T. (2015). The
490 feasibility of using near infrared and Raman spectroscopic techniques to detect
491 fraudulent adulteration of chili powders with Sudan dye. *Food Control*, 48, 75–83.

492 Helton, J. C., & Davis, F. J. (2003). Latin hypercube sampling and the propagation of
493 uncertainty in analyses of complex systems. *Reliability Engineering and System*
494 *Safety*, 81(1), 23–69.

495 ICCO (2017). International Cocoa Organization Daily Prices of cocoa Beans
496 <https://www.icco.org/statistics/cocoa-prices/daily-prices.html>, Consulted: 13th
497 January 2018.

498 Krysiak, W. (2006). Influence of roasting conditions on coloration of roasted cocoa
499 beans. *Journal of Food Engineering*, 77(3), 449-453.

500 Huang, J., Romero, S., & Moshgbar, M. (2010). Practical Considerations in Data Pre-
501 treatment for NIR and Raman Spectroscopy. *American Pharmaceutical Review*,
502 13(6). <http://www.americanpharmaceuticalreview.com>. Consulted: 2 December
503 2017

504 Huang, X. Y., Teye, E., Sam-Amoah, L. K., Han, F. K., Yao, L. Y., & Tchabo, W.
505 (2014). Rapid measurement of total polyphenols content in cocoa beans by data
506 fusion of NIR spectroscopy and electronic tongue. *Analytical Methods*, 6(14),
507 5008–5015.

508 Li, Y., Feng, Y., Zhu, S., Luo, C., Ma, J., & Zhong, F. (2012). The effect of alkalization
509 on the bioactive and flavor related components in commercial cocoa powder.
510 *Journal of Food Composition and Analysis*, 25(1), 17-23.

511 Li, X., Zhang, Y., & He, Y. (2016). Rapid detection of talcum powder in tea using FT-
512 IR spectroscopy coupled with chemometrics. *Scientific Reports*, 6(February),
513 30313.

514 Lohumi, S., Lee, S., Lee, H., & Cho, B. K. (2015). A review of vibrational
515 spectroscopic techniques for the detection of food authenticity and adulteration.
516 *Trends in Food Science and Technology*, 46(1), 85–98.

517 Martens, H., Nielsen, J. P., & Engelsen, S. B. (2003). Light scattering and light
518 absorbance separated by extended multiplicative signal correction. Application to
519 near-infrared transmission analysis of powder mixtures. *Analytical Chemistry*,
520 75(3), 394–404.

521 Miller, K. B., Hurst, W. J., Payne, M. J., Stuart, D. A., Apgar, J., Sweigart, D. S., & Ou,
522 B. (2008). Impact of alkalization on the antioxidant and flavanol content of
523 commercial cocoa powders. *Journal of Agricultural and Food Chemistry*, 56(18),
524 8527–8533.

525 Moore, J. C., Spink, J., & Lipp, M. (2012). Development and Application of a Database
526 of Food Ingredient Fraud and Economically Motivated Adulteration from 1980 to
527 2010. *Journal of Food Science*, 77(4).

528 OLAM (2017). *De Zaan® Cocoa Manual*. The Netherlands: Archer Daniels Midland
529 Company BV.

530 Pérez, É., Lerma, M. J., Fuentes, A., Palomares, C., & Barat, J. M. (2016). Control of
531 undeclared flavoring of cocoa powders by the determination of vanillin and ethyl
532 vanillin by HPLC. *Food Control*, 67, 171–176.

533 Pizarro, C., Esteban, I., Nistal, A.-J., & González, J.-M. (2004). Influence of data pre-
534 processing on the quantitative determination of the ash content and lipids in roasted
535 coffee by near infrared spectroscopy. *Analytica Chimica Acta*, 509, 217–227.

536 Ribeiro, J. S., Ferreira, M. M. C., & Salva, T. J. G. (2011). Chemometric models for the
537 quantitative descriptive sensory analysis of Arabica coffee beverages using near
538 infrared spectroscopy. *Talanta*, 83(5), 1352–1358.

539 Rosa, C. S., Tessele, K., Prestes, R. C., Silveira, M., & Franco, F. (2015). Effect of
540 substituting of cocoa powder for carob flour in cakes made with soy and banana
541 flours. *International Food Research Journal*, 22(5), 2111–2118.

542 Salem, E. M., & Ohaad Fahad, A. A. (2012). Substituting of Cacao by Carob Pod
543 Powder In Milk Chocolate Manufacturing. *Australian Journal of Basic and Applied
544 Sciences*, 6(3), 572–578.

545 Savitzky, A., & Golay, M. (1951). Smoothing and Differentiation of Data by Simplified
546 Least Squares Procedures. *Z. Physiol. Chem. Chem. & Ind*, 40(42).

547 Shankar, M. U., Levitan, C. A., Prescott, J., & Spence, C. (2009). The influence of color
548 and label information on flavor perception. *Chemosensory Perception*, 2(2), 53–58.

549 Stohner, J., Lukas, B., Suter, M., Zucchetti, B., Deuber, F., & Hobi, F. (2012). NIRS of
550 chocolate and its chemometric analysis. *Newfood*, 15(6), 21–28.

551 Sunoj, S., Igathinathane, C., & Visvanathan, R. (2016). Nondestructive determination of
552 cocoa bean quality using FT-NIR spectroscopy. *Computers and Electronics in
553 Agriculture*, 124, 234–242.

554 Talens, P., Mora, L., Morsy, N., Barbin, D. F., ElMasry, G., & Sun, D.-W. (2013).
555 Prediction of water and protein contents and quality classification of Spanish
556 cooked ham using NIR hyperspectral imaging. *Journal of Food Engineering*,
557 117(3), 272–280.

558 Teye, E., & Huang, X. (2015). Novel Prediction of Total Fat Content in Cocoa Beans by
559 FT-NIR Spectroscopy Based on Effective Spectral Selection Multivariate
560 Regression. *Food Analytical Methods*, 8(4), 945–953.

561 Teye, E., Huang, X., Sam-Amoah, L. K., Takrama, J., Boison, D., Botchway, F., &
562 Kumi, F. (2015). Estimating cocoa bean parameters by FT-NIRS and chemometrics
563 analysis. *Food Chemistry*, 176, 403–410.

564 Veselá, A., Barros, A. S., Synytsya, A., Delgadillo, I., Čopíková, J., & Coimbra, M. A.
565 (2007). Infrared spectroscopy and outer product analysis for quantification of fat,
566 nitrogen, and moisture of cocoa powder. *Analytica Chimica Acta*, 601(1), 77–86.

567 Westad, F., Schmidt, A., & Kermit, M. (2008). Incorporating chemical band-assignment
568 in near infrared spectroscopy regression models. *Journal of Near Infrared
569 Spectroscopy*, 16(1), 265.

570 Wold, S., Antti, H., Lindgren, F., & Öhman, J. (1998). Orthogonal signal correction of
571 near-infrared spectra. *Chemometrics and Intelligent*, 44, 175–185.

572 Yousif, A. K., & Alghzawi, H. M. (2000). Processing and characterization of carob
573 powder. *Food Chemistry*, 69(3), 283–287.

574 Zyzelewicz, D., Krysiak, W., Nebesny, E., & Budryn, G. (2014). Application of various
575 methods for determination of the color of cocoa beans roasted under variable
576 process parameters. *European Food Research and Technology*, 238(4), 549–563.

577 **Figure captions**

578

579 **Fig 1.** Score plot of the first and the second principal components of the PCA model
580 using color parameters L^* , C^* , h^* and pH of pure carob and cocoa powder samples
581 (n=18, in triplicate). NC: natural Cocoa; LAC: light alkalized cocoa; MAC: medium
582 alkalized cocoa; SAC: strong alkalized cocoa; LCF: light carob flour; MCF: medium
583 carob flour; DCF: dark carob flour.

584

585 **Fig 2.** Spectra with raw data within the 1100 - 2500 nm range (a) Cocoa. (b) Carob
586 flour.

587

588 **Fig 3.** Second derivative, Savitzky Golay smoothing and orthogonal signal correction
589 pretreated the cocoa (brown) and carob (grey) spectra within the 1100 - 2500 nm range.

590

591 **Fig 4.** The NIR PCA score plot to separate pure cocoa powder and different levels of
592 adulteration with carob flour (high adulteration HA (40-60%), low adulteration LA (0-
593 20%) and medium adulteration MA (20-40%)).

594

595 **Fig 5.** NIR PLS-DA score plot from latent variable 1 and 2, pure cocoa (brown
596 triangles) carob powder (gray squares) and adulterations (blue circles).

597

598 **Fig 6.** Predicted *versus* observed values of the adulterant percentages (n=140) of the
599 pure cocoa and carob powder at different levels of adulterated samples.

Table 1. Color parameters and pH (mean and standard deviation) values for the carob and cocoa pure samples.

Product	Color Parameters			pH \pm sd
	L* \pm sd	C* \pm sd	h* \pm sd	
LCF1	48.6 \pm 0.4 ^{de}	23.6 \pm 0.3 ^e	61.0 \pm 0.3 ^b	5.03 \pm 0.01 ^a
LCF2	47.70 \pm 0.06 ^{de}	24.1 \pm 0.2 ^e	60.98 \pm 0.11 ^b	5.12 \pm 0.01 ^a
LCF3	46.1 \pm 0.2 ^{de}	26.3 \pm 0.7 ^e	61.5 \pm 0.3 ^b	4.67 \pm 0.01 ^a
LCF4	44.17 \pm 0.3 ^{de}	20.7 \pm 0.2 ^e	61.1 \pm 0.3 ^b	4.911 \pm 0.01 ^a
MCF	37.6 \pm 0.4 ^{ab}	16.9 \pm 0.7 ^{bc}	60.2 \pm 0.5 ^a	4.851 \pm 0.01 ^a
DCF	34.5 \pm 1.5 ^a	12.9 \pm 0.9 ^a	60 \pm 2 ^a	4.817 \pm 0.01 ^a
NC1	48.7 \pm 0.2 ^e	20.1 \pm 0.5 ^{de}	58.8 \pm 0.4 ^c	5.391 \pm 0.01 ^a
NC2	48.33 \pm 0.13 ^e	22.3 \pm 0.4 ^{de}	59.5 \pm 0.3 ^c	5.46 \pm 0.01 ^b
NC3	50.3 \pm 0.6 ^e	22.19 \pm 1.02 ^{de}	60.0 \pm 0.4 ^c	5.70 \pm 0.01 ^b
LAC1	42.3 \pm 0.6 ^c	22.4 \pm 0.7 ^{cd}	54.3 \pm 0.4 ^c	6.901 \pm 0.01 ^c
LAC2	44.2 \pm 0.5 ^c	18.63 \pm 1.02 ^{cd}	55.0 \pm 0.9 ^c	6.96 \pm 0.02 ^c
LAC3	41.7 \pm 0.5 ^b	19.80 \pm 0.13 ^{bc}	54.5 \pm 0.5 ^c	6.98 \pm 0.01 ^d
MAC1	44.9 \pm 1.5 ^c	18 \pm 2 ^{cd}	55.7 \pm 0.6 ^c	7.24 \pm 0.01 ^c
MAC2	41.9 \pm 0.7 ^b	18.0 \pm 0.6 ^{bc}	54.2 \pm 0.5 ^c	7.34 \pm 0.03 ^d
MAC3	35.85 \pm 1.05 ^b	16.0 \pm 0.8 ^{bc}	43.0 \pm 0.6 ^c	7.43 \pm 0.01 ^d
SAC1	32.1 \pm 0.8 ^a	11.6 \pm 0.9 ^b	46.5 \pm 0.6 ^c	7.81 \pm 0.01 ^e
SAC2	39.4 \pm 0.5 ^a	19.76 \pm 0.99 ^b	51.4 \pm 0.8 ^c	7.84 \pm 0.01 ^e
SAC3	40.1 \pm 0.2 ^a	17.3 \pm 0.8 ^b	53.2 \pm 0.6 ^c	7.92 \pm 0.01 ^e

Values in the same column followed by the same letter(s) are not significantly different according to ANOVA at a 95% Confidence level. For cocoas (N): Natural cocoa (NC), light alkalized cocoa (LAC), medium alkalized cocoa (MAC) and strong alkalized cocoa (SAC). For carob flours (A): light carob flour (LCF), medium carob flour (MCF) and dark carob flour (DCF).

Table 2. Results for classification accuracy of the PLS-DA model

	Cocoa	Carob	Adulterated	Classification
Cocoa	7	0	0	100%
Carob	0	4	0	100%
Adulterated	0	0	32	100%

Table 3. Results of the PLS models constructed for the prediction of carob flour content in cocoa powders.

Pre-treatment	#LV	Calibration			Cross-validation				Prediction				
		R^2_c	RMSEC	Slope	R^2_{cv}	RMSECV	Bias	Slope	R^2_p	RMSEP	Bias	Slope	RPD
Raw data	7	0.951	4.5	0.951	0.945	4.8	0.019	0.951	0.961	4.4	0.197	0.968	4.7
2 nd Der. S-G	4	0.969	3.6	0.969	0.965	3.8	0.013	0.968	0.969	3.9	0.711	0.998	5.2
OSC	1	0.975	3.2	0.975	0.975	3.2	0.006	0.976	0.974	3.6	0.474	0.992	5.8
2 nd Der. S-G + OSC	1	0.980	2.9	0.981	0.979	2.9	0.006	0.981	0.974	3.2	0.626	1.004	6.3

2nd Der. S-G = Second derivative-Savitzky Golay; OSC = Orthogonal signal correction; #LV = latent variables; R^2_c = coefficient of determination for calibration; RMSEC = root mean square error of calibration; R^2_{cv} = coefficient of determination for cross-validation; RMSECV = root mean square error of cross-validation; R^2_p = coefficient of determination for prediction; RMSEP = root mean square error of prediction; Bias = estimation of the difference between the experimental value and NIR predictions; RPD = ratio of prediction deviation.

Figure 1

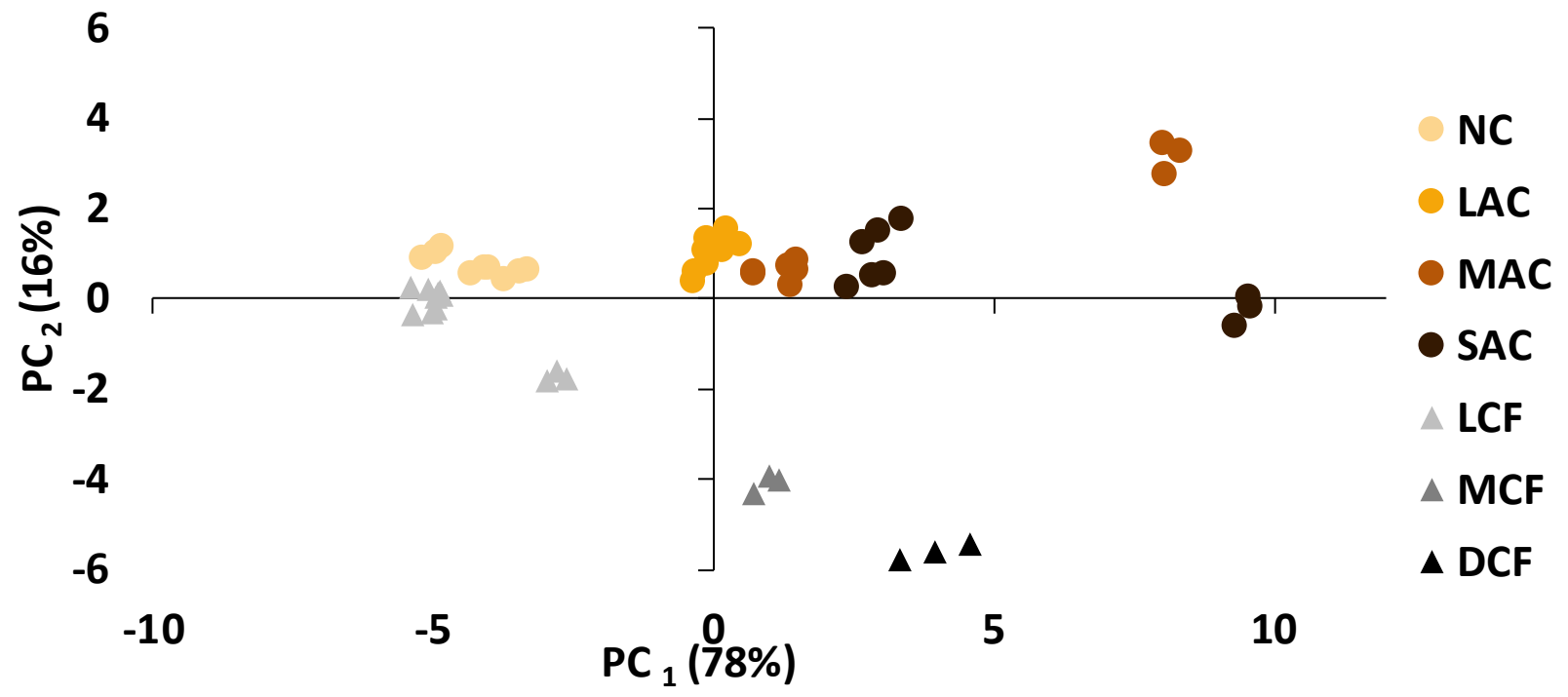


Fig 1. M.A. Quelal et al.

Figure 2

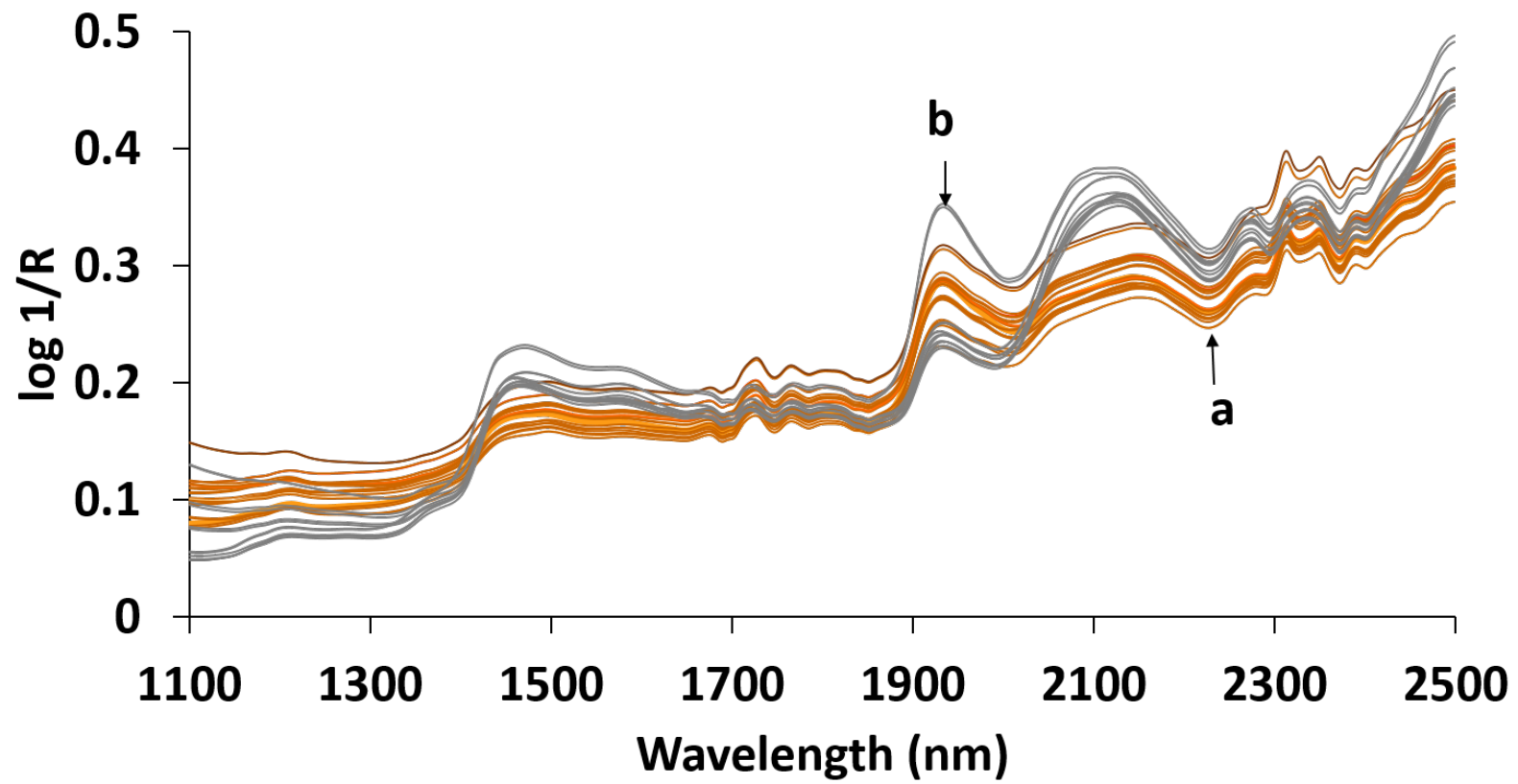


Fig 2. M.A. Quelal et al.

Figure 3

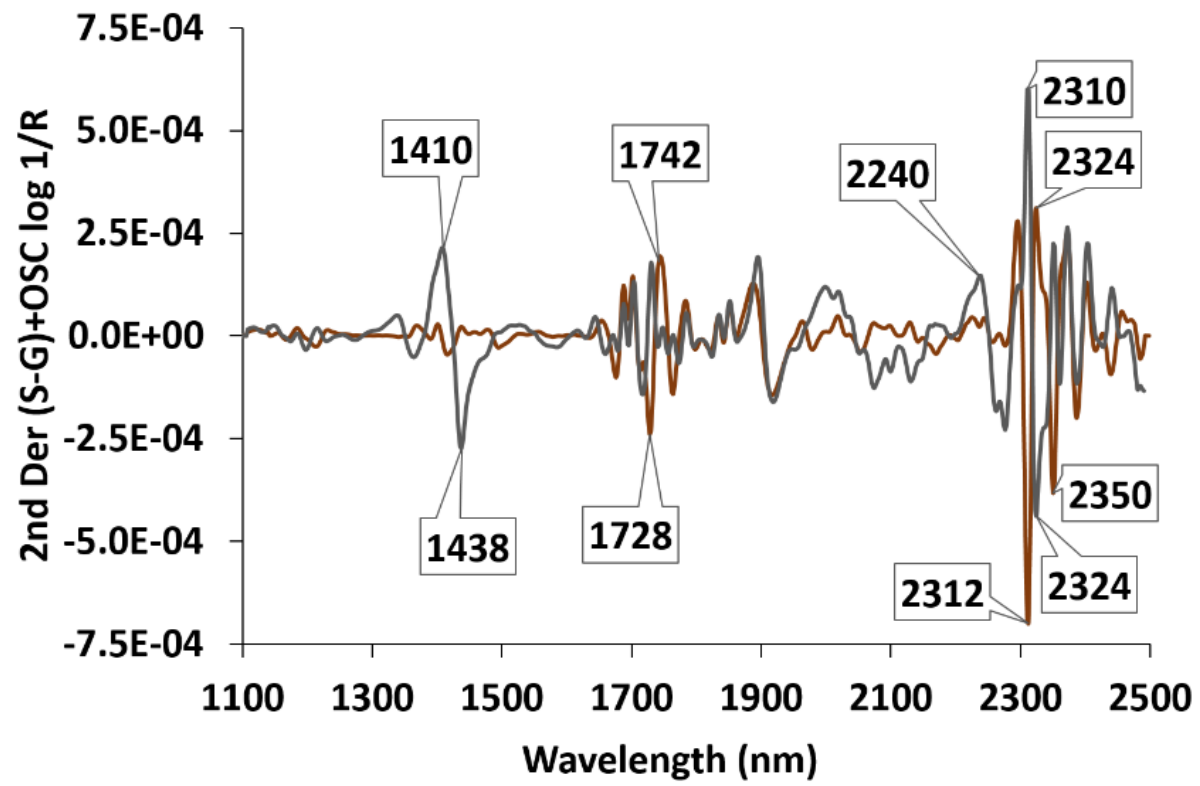


Fig 3. M.A. Quelal et al.

Figure 4

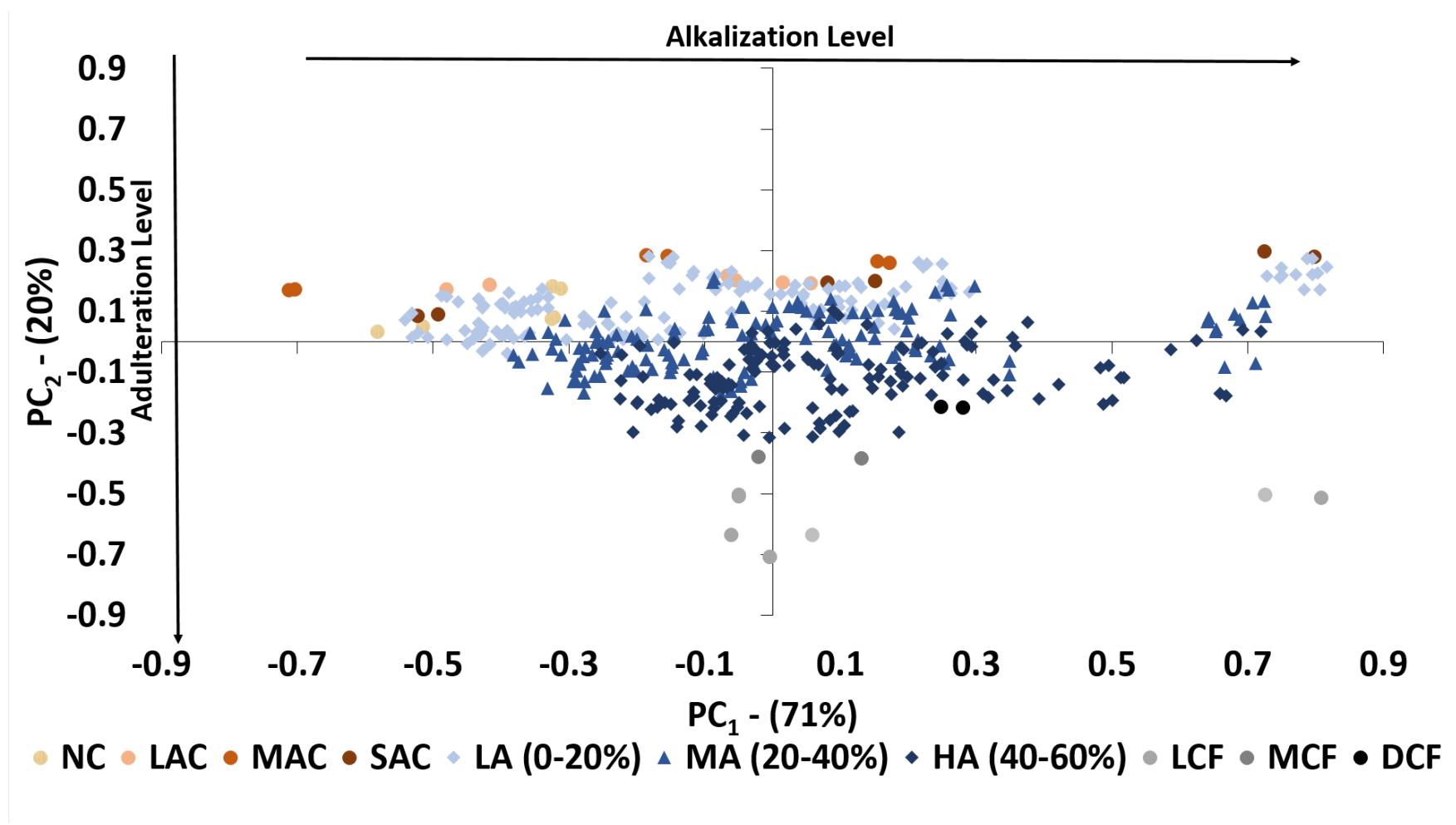


Fig 4. M.A. Quelal et al.

Figure 5

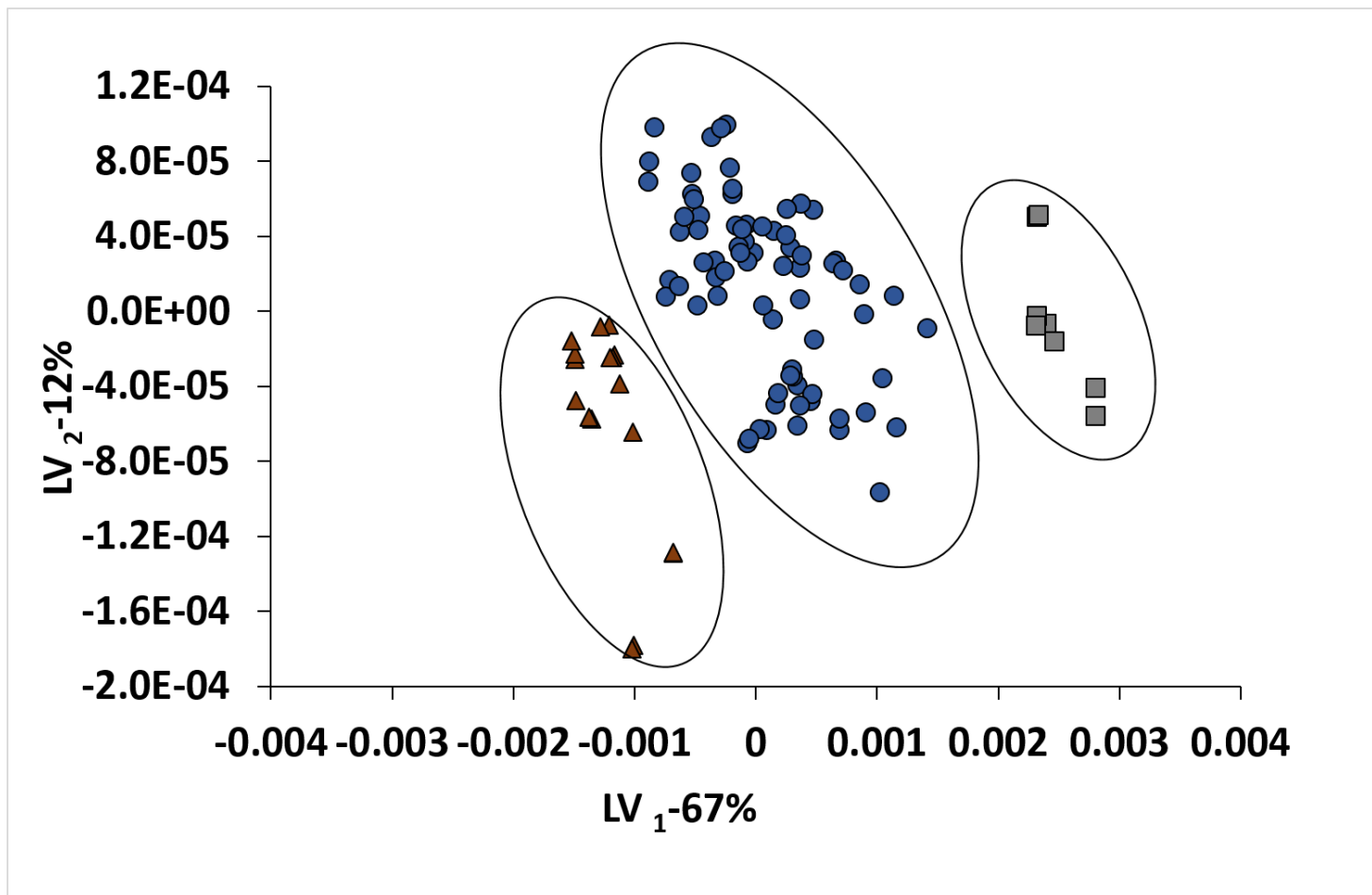


Fig 5. M.A. Quelal et al.

Figure 6

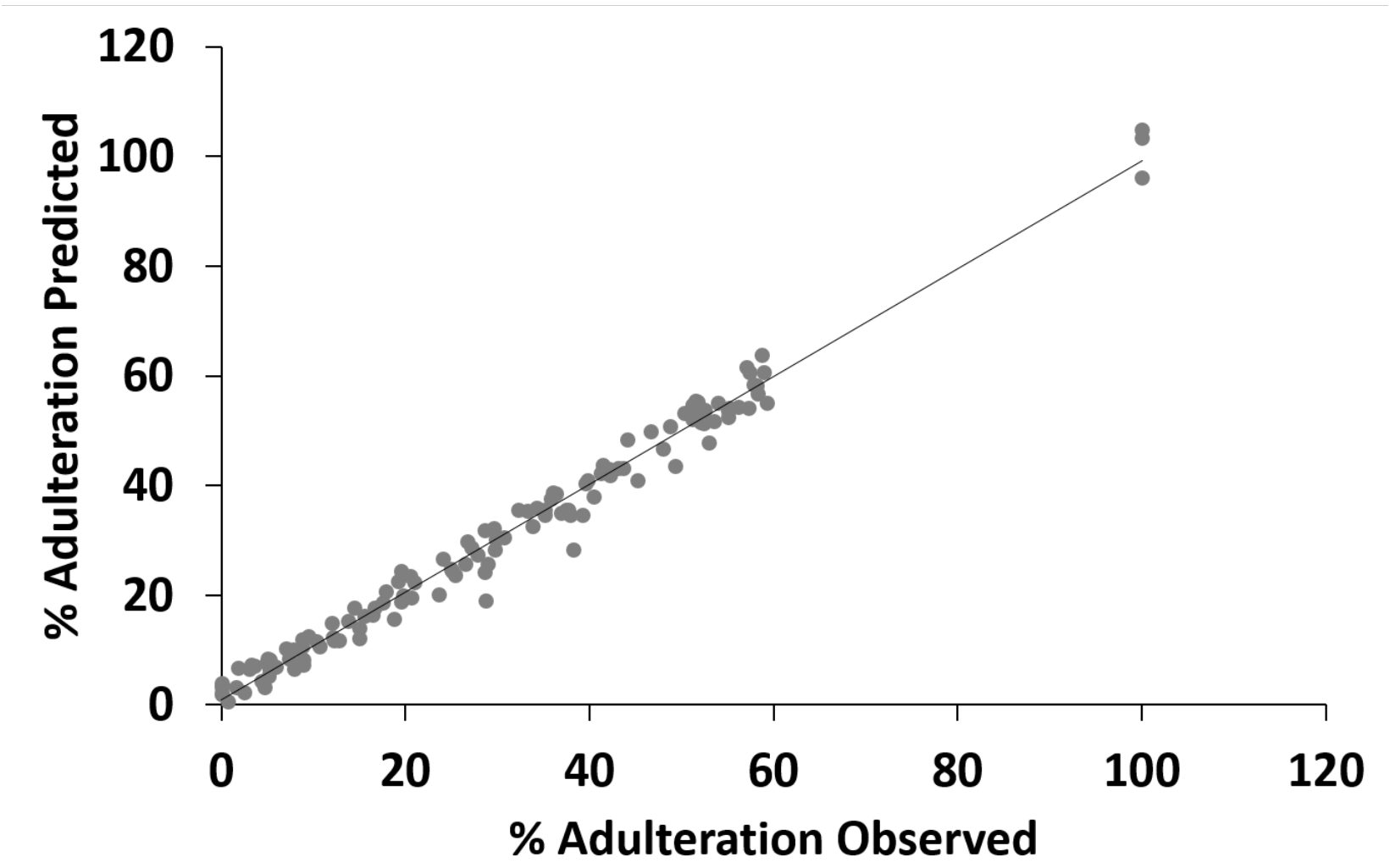


Fig 6. M.A. Quelal et al.

Highlights

- Near infrared spectroscopy can detect cacao adulterated with carob flour
- The method is rapid, useful and simple for quality cacao analyses
- PLS-DA distinguishes pure cocoa powders from those adulterated with carob flour
- A PLS analysis has the potential to quantify the percentage of adulteration